18. MAGNETIC PROPERTIES OF LEG 37 BASALTS AND A DETERMINATION OF PALEOMAGNETIC FIELD INTENSITY

D.J. Dunlop and C.J. Hale, Geophysics Laboratory, University of Toronto, Toronto, Canada

ABSTRACT

We report NRM, AF and thermal demagnetization, VRM, hysteresis, Curie temperature, and paleointensity data for 23 samples from DSDP Leg 37. Samples from Hole 332B have low inclinations (1.5° to 34°, predominantly negative) for this latitude, whereas Site 335 samples have more normal values (-42° to -54°). NRM is usually stable in direction during AF demagnetization to 1000 oe and thermal demagnetization to 250°C. In a two-month storage test, NRM changed 5° or less in six samples, about 10° in three samples, and 20-25° in three samples. Although VRM is not large at 20°C, it frequently increases to a spectacular peak at 75°-100°C, a Hopkinson effect reflecting low Curie points. The relaxation times involved would produce both accelerated viscous magnetization over the time of a polarity epoch and an enhanced axial anomaly due to the higher susceptibility of hot material rising at a mid-ocean ridge.

There is a striking correlation among NRM stability, hysteresis properties, the presence or absence of a VRM peak around 100°C, and thermomagnetic curves. Magnetically soft samples contain coarse, multidomain titanomagnetite with a Curie point of about 200°C. This phase is chemically stable on heating and is responsible for VRM. Magnetically hard samples contain in addition a single-domain-like phase with Curie temperature 450°-520°C, presumably the result of exsolution of originally homogeneous titanomagnetite. The amount of this hard phase increases two- or three-fold upon heating.

Five samples were successfully studied by the Thellier-Thellier method. No meaningful data were obtained above 200°C because of chemical changes. The paleofield intensity estimates fall in the range 0.10 to 0.45 oe.

STABLE MAGNETIZATION

AF Demagnetization of NRM

Three samples (332B-11-4, 332B-36-3, 335-8-4) were stepwise AF demagnetized to 1000 oe using a 3-axis Schonstedt demagnetizer. Magnetizations were measured with a Digico spinner magnetometer. Data are listed in Table 1. These samples were directionally stable to 800 or 1000 oe.

Seven samples (2-1, 3-1, 11-2, 29-1, 44-6 from Hole 332B; 20-2 from Site 334; and 6-1 from Site 335) were AF demagnetized to 2500 oe and measured along a single-axis, using an instrument described by West and Dunlop (1971). Median demagnetizing fields, $H_{1/2}$ varied from 34 oe for 332B-11-2 to 685 oe for 335-6-1. (See Table 2 for a complete listing).

Storage Test of NRM

Twelve samples (11-1, 14-2, 17-1, 22-4, 27-2, 33-1, 46-2 from Hole 332B; 26-1 from Site 334; 7-1, 8-2, 10-1, 12-3 from Site 335) were stored two months with the present earth's field parallel to the vertical up axis of each core. Data are tabulated in Table 3. Five 332B samples were stable (NRM changed 5° or less), two were less stable (NRM changed 20°-25°). Three 335 samples changed about 10°, the other 25°. Sample 334-26-1 was very stable in direction.

Thermal Demagnetization of NRM

After storage, the above samples were thermally demagnetized in field-free space. Measurements were made with a PAR spinner magnetometer. Heatings were in vacuum (10^{-5} torr), but irreversible chemical changes nevertheless occurred above 250°C. Up to this temperature, NRM was generally stable in direction. Three examples are shown later in Figure 3. Complete data are tabulated in Table 4.

Direction and Intensity of NRM

NRM intensities are in the range 1000-4000 $\times 10^{-6}$ emu cm^{-3}, sufficient to account for magnetic anomalies observed at the ocean surface. However, Hole 332B samples have anomalously low inclinations, 1.5° to 34°, for their age and latitude. As expected from their location in a negative anomaly (between positive anomalies 2 and 3), they tend to be reversely magnet-

TABLE 1
AF Demagnetization of DSDP Leg 37 Basalts

A. C. Field	$M \times 10^6$	D	I
332B-11-4, 60-73 (51) DP DP			
0	4535	268.0	+8.1
25	4365	264.5	+11.3
50	4040	262.6	+15.3
75	3400	264.7	+17.4
100	2880	261.7	+18.2
150	2040	266.0	+21.6
200	1535	267.1	+23.0
250	1220	267.0	+23.2
300	2275	351.2	+3.6
350	1420	348.2	+5.4
400	1010	343.5	+7.4
500	1360	349.1	+5.4
600	630	339.2	+10.7
800	562	344.4	+3.9
1000	353	338.1	+2.5
332B-36-3, 123-135 (6A) DP DP			
0	4140	43.9	+2.4
25	4120	42.5	+2.5
50	4250	39.8	+1.9
100	4280	42.0	+2.1
150	3950	43.1	+2.7
200	3690	42.2	+2.3
250	3170	42.4	+2.9
300	2755	39.2	+2.8
400	2265	41.0	+2.0
500	1650	43.9	+3.6
600	1275	43.5	+4.0
800	844	44.0	+3.8
1000	488	39.6	−8.5
335-8-4, 14-26 (P1B) DP DP			
0	4630	21.0	−54.8
25	4620	27.6	−54.2
50	4660	21.9	−53.4
100	4670	21.1	−55.4
150	4690	20.6	−54.1
200	4620	20.0	−54.5
250	4300	20.7	−53.7
300	4040	25.3	−52.5
400	3200	20.5	−53.5
500	2540	18.9	−52.7
600	2050	19.5	−53.5
800	1275	18.3	−51.5
1000	897	19.1	−47.3

Note: Results above 250 oersteds are likely spurious. The apparent intensity increase and jump in D are artifacts occasionally generated by the Digico magnetometer.

ized, but some normal magnetizations occur. Some normally magnetized cores are obviously viscous (e.g., 332B-11-1, 11-4), others, however, are not (e.g., 332B-36-3, 46-2). On AF demagnetization, both 11-4 and 36-3 retain positive inclinations to 800 oe, while 11-1 and 46-2 change to negative inclinations during thermal demagnetization. On this evidence, it is difficult to decide whether the reversals are real or a result of VRM during the present polarity epoch. The effect, in either case, is to reduce the magnetic anomaly. Samples from Site 335 are reversely magnetized with inclinations of -42° to -55°.

UNSTABLE MAGNETIZATION

VRM Decay — 20°C to 200°C

The relaxation times examined in laboratory VRM experiments vary from seconds to days, or at the most months. The usual method of assessing the effect of VRM over the 10^6 yr duration of a polarity epoch is to extrapolate from the laboratory viscosity coefficient, S, using the experimental relationship

$$J_r(t) = J_r(t_o) + S(\log t - \log t_o)$$

where J_r is remanence measured at t or t_o. This is an uncertain procedure because S is not constant, but depends on the distribution of relaxation times τ for a particular sample.

It is a simple matter to activate the appropriate range of τ by taking advantage of the fact that τ is temperature dependent. Since

$$\tau \propto \exp[\text{const } K(T)/T]$$

(Néel, 1949), where the anisotropy constant K decreases with temperature T, i.e., very large values of τ at 20°C are accessible in a VRM experiment carried out only slightly above room temperature.

Table 5 lists viscosity coefficients determined by measuring the time decay of a VRM acquired by 10 min exposure to a 2-oe field at temperatures of 20°C to 200°C. Almost invariably S increases with temperature. In some samples, S peaks at 75°-100°C. An example is shown in Figure 1, where the lines join values of VRM measured at equal decay times in the range 10-300 sec. (The actual experiments covered a much broader time scale.) The peak is a Hopkinson effect, reflecting the low Curie temperatures of these samples (cf. Figure 2).

Enhancement of VRM and Susceptibility

A peak in S at these temperatures indicates an abundance of relaxation times in the range 10^5-10^6 yr compared to those in the sec to yr range. Viscous magnetic effects are therefore accelerated over the time of a polarity epoch relative to extrapolations from laboratory data.

A Hopkinson peak in S implies a peak in susceptibility at similarly low temperatures. Dunlop (1974) has suggested thermal enhancement of induced magnetization in the deep continental crust as a source of regional magnetic anomalies. Although submarine basalts usually have a high Q (remanent/induced magnetization ratio), a similar enhancement of susceptibility could be significant for hot basaltic magma rising at a ridge axis and could in part explain why axial anomalies tend to be high compared to the other magnetic stripes.

MAGNETIC MINERALS AND DOMAIN STRUCTURE

Hysteresis Measurements

Near-saturation hysteresis was measured for the 10 samples whose VRM at 200°C had previously been in-

TABLE 2
Hysteresis, NRM, and Viscosity Data

Sample (Core-Section)	$J_{nrm} \times 10^6$ (1-axis)	$(J_s)_o$	S_o/J_{so} $\times 10^6$	S_{100}/J_{so} $\times 10^6$	$\tilde{H}_{1/2}$	$(H_c)_o$	$(H_c)_{200}$	$(H_{cr})_o$	$(H_{cr})_{200}$	$\left(\frac{H_{cr}}{H_c}\right)_o$	$\left(\frac{H_{cr}}{H_c}\right)_{200}$	$\left(\frac{J_{rs}}{J_s}\right)_o$	$\left(\frac{J_{rs}}{J_s}\right)_{200}$
Hole 332B													
2-1	755	3.69	2.1	–	350	261	80	445	153	1.70	1.92	0.385	0.192
3-1	20	4.92	1.6	3.2	35	110	79	180	153	1.64	1.95	0.244	0.169
11-2	840	1.86	23.4	132.0 (75°C)	34	13	47	80	109	6.12	2.32	0.012	0.136
11-4	37	1.80	3.5	40.2	135	88	180	158	284	1.80	1.58	0.220	0.403
29-1	825	1.53	4.1	15.6	245	81	83	146	128	1.80	1.54	0.201	0.263
36-3	79	0.93	3.3	6.8	412	216	296	585	501	2.71	1.69	0.290	0.512
44-6	640	2.13	12.5	75.8	42	39	80	145	157	3.72	1.96	0.113	0.196
Site 334													
20-2	345	0.53	5.8	14.7	350	163	153	230	195	1.41	1.27	0.443	0.408
Site 335													
6-1	2940	3.72	0	0	685	214	325	450	467	2.10	1.44	0.354	0.437
8-4	3130	5.10	1.8	6.7	538	333	210	435	324	1.30	1.54	0.506	0.452
10-1	3180	5.61	?	?	?	232		425		1.83		0.231	

Note: Hysteresis was measured on virgin material and again after heating in air to 200°C. All magnetizations are in emu cm^{-3} and fields in oersteds. Symbols defined in the text. 1 - axis refers to long axis only.

vestigated using a ballistic magnetometer and a 2300 oe solenoid. For comparison, saturation hysteresis was measured using virgin chips of the same samples with a PAR vibrating-sample magnetometer in the 20,000 oe field of an electromagnet. Table 1 lists values of saturation magnetization J_{s}, coercive force H_{c}, remanent coercive force H_{cr}, saturation remanence ratio J_{rs}/J_{s} and coercivity ratio H_{cr}/H_{c}, as well as 20°C and 100°C viscosity coefficients normalized to J_{s}. Hysteresis parameters, particularly H_{c}, J_{rs}/J_{s}, and H_{cr}/H_{c}, have diagnostic value in determining domain structure (see e.g., Nagata et al., 1972; Gose et al., 1972). Very low values of J_{rs}/J_{s}, for example in 332B-11-2 and 44-6, indicate multidomain structure. Values near 0.5 (e.g., 335-8-4 and 334-20-2) indicate single-domain grains. The other samples have either a mixture of single-domain and multidomain material or else grain sizes in the pseudo-single-domain range (0.05-20 μm in magnetite). These conclusions probably apply to the carriers of NRM because H_{c} correlates reasonably well with NRM median demagnetizing field $\tilde{H}_{1/2}$.

Thermomagnetic Analysis

Figure 2 illustrates the various types of J_{s} versus T curves recorded with a PAR vibrating sample magnetometer. A few samples, of which 332B-44-6 is an example, exhibit a single low Curie temperature in the range 150°-200°C. Their thermomagnetic curves are nearly reversible upon cooling from 650°C. To judge by the low Curie temperature, the magnetic phase is responsible in a high-titanium titanomagnetite. The multidomain hysteresis properties imply a grain size greater than 20 μm.

Most thermomagnetic curves are irreversible. The saturation magnetization increases after a heating-cooling cycle, often two or threefold. Some examples are 332B-29-1 and 335-17-1, 6-1 in Figure 2. Generally there is evidence for two distinct magnetic phases, a low Curie temperature phase evident in the heating curves and a higher Curie temperature phase whose amount increases irreversibly during heating above 350°-400°C at the expense of the low T_c phase. These samples have more single-domain-like hysteresis properties before and especially after heating (Table 1). That is, both magnetic phases have a finer grain size than the single phase in reversible samples.

The obvious explanation of the irreversible magnetic behavior is that initially homogeneous, moderate to high Ti titanomagnetites exsolve during heating to intergrown ilmenite and low Ti, high Curie temperature titanomagnetite. However, in a few samples, of which 335-6-1 is representative, high T_{c} and low T_{c} phases are seen on both heating and cooling. Irreversible changes occur whether heatings are carried out at near atmospheric oxygen partial pressure or in a hard vacuum.

Correlation of Curie Points, Hysteresis, and VRM

Table 6 illustrates the strong correlation among thermomagnetic, hysteresis, and viscosity data. Type 1 materials (332B-11-1, 11-4, 44-6, for example) possess a single low Curie temperature, soft multidomain hysteresis, high room-temperature viscosity coefficients (relative to saturation magnetization), and Hopkinson-type VRM peaks just below the Curie point. The concentration of NRM at low blocking temperatures and relatively reversible thermomagnetic behavior make these preferred samples for paleointensity determination. Type 2 materials are magnetically harder; however, because much of the NRM is carried by the high T_c phase whose blocking temperatures lie in the range where the sample alters irreversibly, these materials are less favorable for paleointensity determination.

Determination of Magnetic Paleofield Intensity

Paleointensity determination is made difficult in the samples examined as irreversible alteration takes place at not very elevated temperatures. Successful results

TABLE 3
Storage Test – DSDP Leg 37 Basalts

	$M \times 10^6$	D	I
332B-11-1, 115-118 (2) DP DP			
NRM before	1690	305.0	+1.2
NRM after	2125	295.6	−19.9
332B-14-2, 84-86 (2) DP DP			
NRM before	525	31.3	−6.8
NRM after	447	28.9	−8.4
332B-17-1, 6-8 (1) DP DP			
NRM before	3020	137.4	−31.3
NRM after	3610	143.9	−27.1
332B-22-4, 74-77 (5F) DP DP			
NRM before	2040	224.7	−34.1
NRM after	5760	221.0	−9.9
332B-27-2, 101-103 (7D) DP DP			
NRM before	935	263.9	−1.4
NRM after	1035	261.9	−4.9
332B-33-1, 127-130 (1) P13 DP DP[a]			
NRM before	1540	25.5	−11.8
NRM after	1332	19.1	−16.4
332B-46-2, 32-34 DP DP			
NRM before	1955	33.7	+4.7
NRM after	2115	30.8	+3.5
333-26-1, 141-143 P18 DP DP			
NRM before	1430	281.3	−21.6
NRM after	1472	277.5	−21.8
335-7-1, 85-87 (3B) DP DP			
NRM before	2510	135.0	−48.4
Nrm after	4075	128.1	−58.1
335-8-2, 24-26 (3) DP DP			
NRM before	2030	8.5	−50.4
NRM after	2643	3.1	−57.9
335-10-1, 22-24 (1E) DP DP			
NRM before	2050	62.9	−42.6
NRM after	3903	62.7	−67.7
335-12-3, 132-134 (7A) DP DP			
NRM before	1720	27.8	−47.8
NRM after	2608	21.2	−57.5

Note: Samples were stored 2 months with their vertical up (I = −90°) axes in the direction and sense of the present Earth's field. NRM measured before and after storage.

[a]The core itself is labelled 332B-37-1.

TABLE 4
Thermal Demagnetization of DSDP Leg 37 Basalts

Temperature	$M \times 10^6$	D	I
332B-11-1, 114-118 (2) DP DP			
20	1602	304.7	−7.1
75	1359	300.4	−3.1
125	910	298.4	+6.7
175	640	298.8	−11.9
200	695	298.5	−2.4
250	863	294.2	−5.9
332B-14-2, 84-86 (2) DP DP			
20	384	326.5	−0.3
75	408	324.8	−11.2
125	424	327.9	−10.6
175	408	334.8	−15.0
200	589	325.8	+35.5
250	511	330.2	+26.7
332B-22-4, 75-77 (5F) DP DP			
20	4980	222.4	−10.9
100	4920	222.0	−10.8
175	4840	222.5	−8.8
250	6540	222.3	−10.9
300	4900	222.9	−4.0
332B-27-2, 101-103 (7D) DP DP			
20	885	265.7	−2.5
75	839	265.7	−2.6
125	781	268.4	−4.8
175	771	274.4	−9.7
200	730	274.2	+1.0
250	652	280.0	−16.0
332B-33-1, 127-130 (1) P13 DP DP[a]			
20	1183	27.1	−31.9
75	1160	29.0	−33.0
125	1125	27.3	−32.9
175	908	24.8	−18.8
200	798	33.1	−26.4
250	646	30.4	−39.1
332B-46-2, 32-34 DP DP			
20	821	43.1	−67.2 (?)
50	1705	30.3	−9.3
100	11,140	283.7	+80.7 (?)
335-7-1, 85-87 (3B) DP DP			
20	3400	144.7	−62.0
50	3380	141.1	−59.8
100	2850	180.0	+85.5 (?)
335-10-1, 22-24 (1E) DP DP			
20	3450	64.9	−67.0
75	3350	66.2	−66.2
125	3325	64.7	−67.9
175	2705	64.8	−67.6
200	2715	63.7	−65.8
250	2980	64.9	−66.0

[a]The core itself is labelled 37-1.

TABLE 5
Magnetic Viscosity Coefficients Measured at Various Temperatures

Sample (Core-Section)	S × 10^6 (emu cm^{-3} $logcycle^{-1}$) 20°C	50°C	75°C	100°C	150°C	200°C
Hole 332B						
2-1	7.8	7.8	7.8	–	–	–
3-1	7.9	11.0	–	15.7	26.7	47.6
11-2	43.5	210.8	245.8	137.5	49.5	83.3
11-4	6.3	9.4	34.3	72.4	25.7	18.6
29-1	6.3	14.1	17.3	23.9	34.9	18.6
36-3	3.1	9.4	11.0	6.3	–	–
44-6	26.7	90.4	114.4	161.4	58.0	22.3
Site 334						
20-2	3.1	6.3	4.6	7.8	22.3	15.9
Site 335						
6-1	0	0	0	0	0	0
8-4	9.4	9.4	20.7	34.3	32.5	20.7

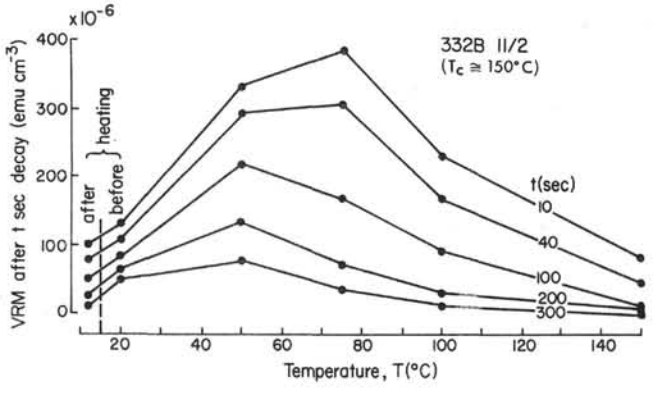

Figure 1. *VRM as a function of decay time and temperature for Sample 332B-11-2. VRM's were produced at the temperatures indicated by 10 min exposure to a 2-oe field. VRM is acquired (and decays) very rapidly at 75°C, just below the Curie temperature of this sample (Hopkinson effect). The vertical dashed line indicates the estimated in-situ temperature (14.5°C) at the depth where 332B-11-2 was sampled.*

were obtained, however, for five samples using the method of Thellier and Thellier (1959). Samples were alternately heated to successively higher temperatures in a zero field and in a laboratory field applied along the vertically up axis. After each heating the sample was remeasured with a PAR SM2B spinner magnetometer. Zero field was held to less than a few gammas and the applied field to 5×10^4 gammas by means of a molypermalloy shielded room containing a triaxial Helmholtz feedback balancing system. Samples were heated in a vacuum of less than 10^{-5} torr. Temperatures in companion heatings were reproduced accurately by means of a Hewlett-Packard temperature programmer.

Paleointensity data for the five samples (332B-11-1, 22-4, 27-2, 33-1; 335-10-1) are presented in Table 4. NRM lost is plotted against PTRM (partial thermoremanent magnetization) gained in Figure 3.

Despite the hard vacuum, chemical alteration was observed at varying temperatures in all five samples. The five samples may be broadly divided into two categories: those (332B-11-1, 33-1; 335-10-1) which appear to be stable to only 175°C and those (332B-22-4, 27-2) which remain stable up to 250°C. Indicated values of H tend to be lower for samples which show alteration at lower temperatures. This may result in part from artificially high PTRM's resulting from formation of secondary magnetite by exsolution upon heating. Samples in the higher stability category (332B-22-4, 27-2) indicate paleointensities which approach more closely the present earth's field intensity. It should be noted that directions for these samples remain stable well after the intensities have become unreliable.

Low oxidation state titanomagnetites present a challenge for paleointensity work because, with reasonable temperature intervals (50°C or so), few reliable points result and these represent only the initial portion of the normal Thellier-Thellier plot, particularly for Type 2, highly alterable materials. Type 1 materials, on the other hand, possess a concentration of low Curie temperatures and a high susceptibility to viscous magnetization which would ordinarily lead them to be considered unsuitable for paleointensity work.

TABLE 6
Correlations Among Hysteresis, NRM, Viscosity, and Thermomagnetic Data

Hole	Sample (Core-Section)	$(H_c)_o$	$\left(\frac{H_{cr}}{H_c}\right)_o$	$\left(\frac{J_{rs}}{J_s}\right)_o$	$\tilde{H}_{1/2}$	$\frac{S_o}{(J_s)_o} \times 10^6$	$\frac{S_{100}}{S_o}$	$\frac{(J_s)_{600}}{(J_s)_o}$	Curie Temperatures
332B	11-2	13	6.12	0.012	34	23.4	5.65*	1.03	≈ 150 (h, c)
332B	44-6	39	3.72	0.113	42	12.5	6.05	1.18	160-180 (h, c)
332B	29-1	81	1.80	0.201	245	4.1	3.80	1.48	220-260 (h) 400-450 (h, c)
332B	11-4	88	1.80	0.220	135	3.5	11.50	1.26	150-200 (h, c)
332B	3-1	110	1.64	0.244	35	1.6	2.00	1.51	250-300 (h, c) 480-500 (h, c)
334	20-2	163	1.41	0.443	350	5.8	2.55	1.60	250-300 (h) 450-480 (c)
335	6-1	214	2.10	0.354	685	0	–	3.64	250-300 (h, c) 500-520 (h, c)
332B	36-3	216	2.71	0.290	412	3.3	2.05	2.12	broad range (h) ≈ 150 (c) 440-460 (c)
332B	2-1	261	1.70	0.385	350	2.1	–	2.83	250-300 (h) 500-550 (c)
335	8-4	333	1.30	0.506	538	1.8	3.70	2.48	240-260 (h) 450-490 (c)

Note: h = heating; c = cooling; * = S_{75}/S_0. All magnetizations are in emu cm^{-3}, all fields are in oersteds, Curie temperatures are in °C. Symbols defined in text.

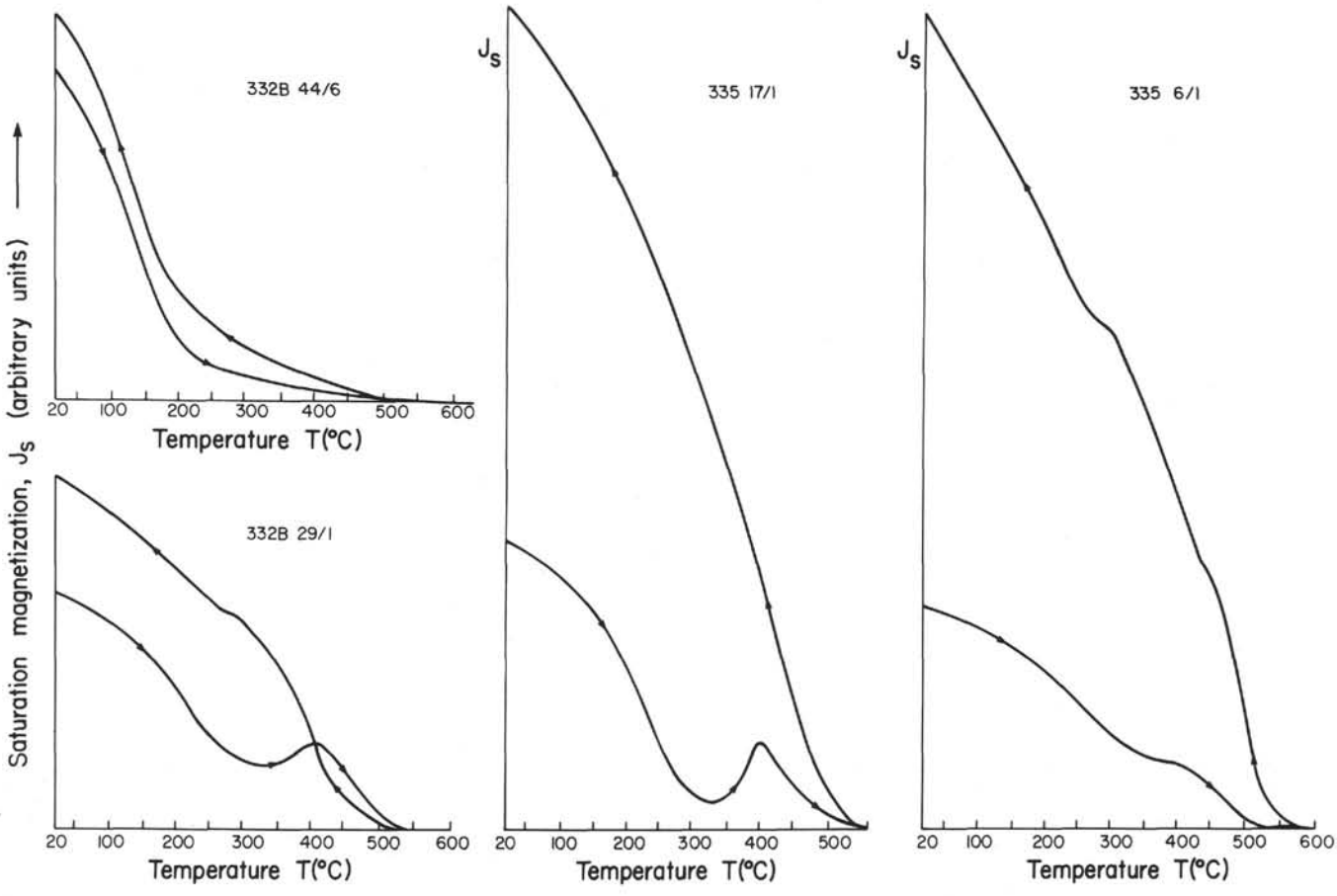

Figure 2. *Typical thermomagnetic (saturation magnetization versus temperature) curves. Notice the reversible curve and single low Curie point of Sample 332B-44-6. This has been designated Class 1 behavior (see text). Production of a high Curie temperature phase during heating to 350°-400°C is evident in both 332B-29-1, whose behavior is nearly reversible, and 335-17-1 which is highly reversible. 335-6-1 is unusual in that it shows two Curie points in both heating and cooling curves.*

TABLE 7
Paleofield Intensity Determined by a Modified Thellier-Thellier Technique

Sample	Temperature Range Used (°C)	Paleofield Intensity H_a (oe)
Hole 332B		
11-1	20-200	0.10 $^{+0.22}_{-0.02}$
22-4	20-175	0.35 $^{+0.05}_{-0.08}$
27-2	20-200	0.45 $^{+0.08}_{-0.07}$
33-1	20-175	0.12 $^{+0.0}_{-0.02}$
Site 335		
10-1	20-200	0.30 $^{+0.06}_{-0.20}$

Note: The best estimate of H_a is derived from least squares fitting to the data (Figure 3). Upper and lower bounds for H_a are determined from lines of maximum and minimum slope through two or more of the data points.

Clearly any total TRM or ARM method of paleointensity determination which involves a single heating to high temperature would be completely unreliable in dealing with low-oxidation state submarine basalts.

ACKNOWLEDGMENTS

This research was supported by the National Research Council of Canada through a D.A.G.S. grant to D.J. Dunlop. We wish to thank G.W. Pearce and D.W. Strangway for the use of their laboratory equipment and for helpful advice on paleointensity determinations based on their experience with lunar materials.

REFERENCES

Dunlop, D.J., 1974. Thermal enhancement of magnetic susceptibility: J. Geophys., v. 40, p. 430-451.

Gose, W.A., Pearce, G.W., Strangway, D.W., and Larson, E.E., 1972. Magnetic properties of Apollo 14 breccias and their correlation with metamorphism: Third Lunar Sci. Conf. Proc., Geochim. Cosmochim. Acta, v. 3, p. 2387-2395.

Nagata, T., Fisher, R.M., and Schwerer, F.C., 1972. Lunar rock magnetism: The Moon, v. 4, p. 161-186.

Néel, L., 1949. Théorie du traînage magnétique des ferromagnétiques en grains fins avec applications aux terres cuites: Ann. Géophys., v. 5, p. 99-136.

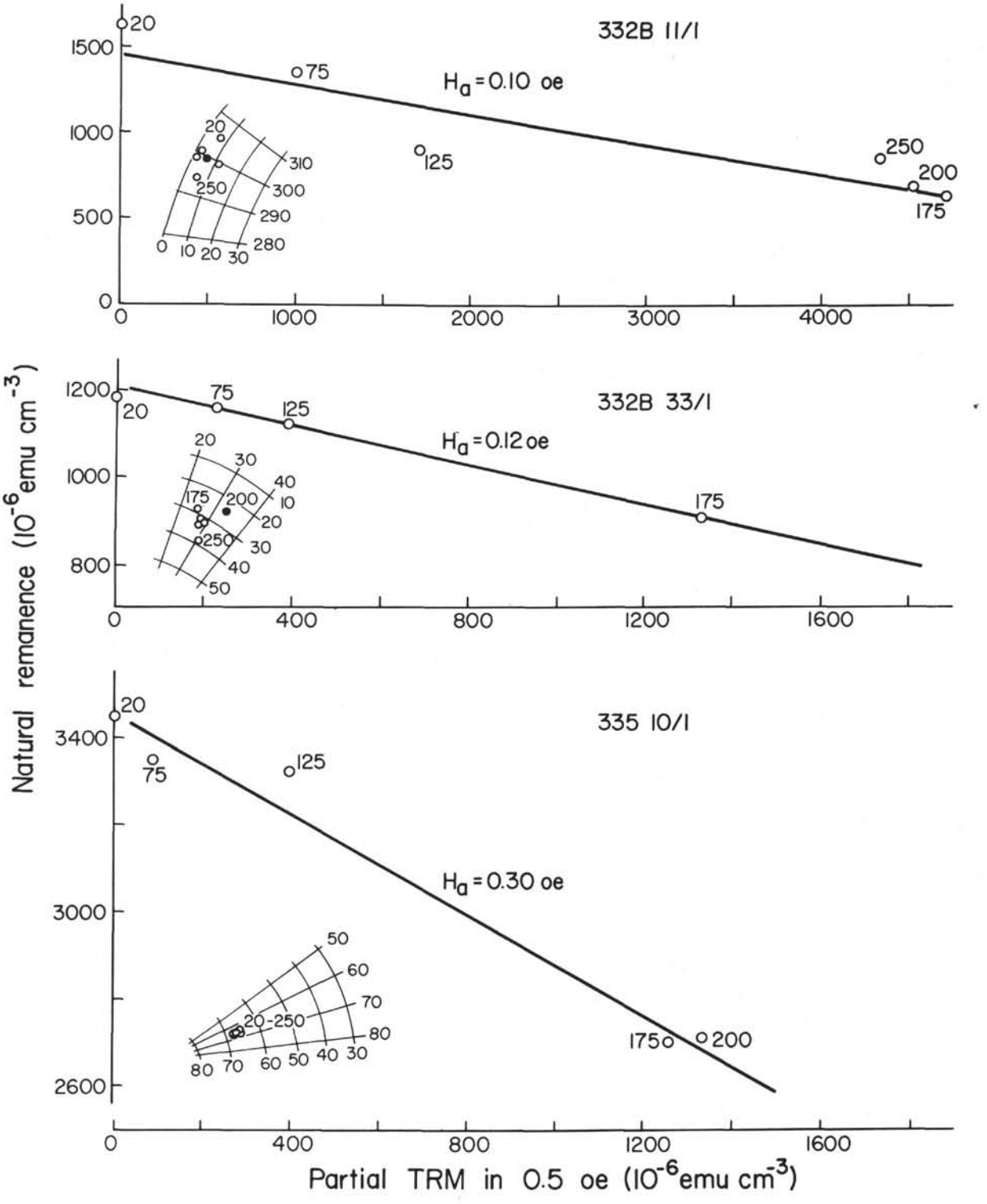

Figure 3. *Thellier and Thellier-type paleointensity determinations. Directional data are plotted on equal-area projections with open circles for upwards or negative inclinations. Directions often remain stable above 175° or 200°C even though chemical alteration has rendered intensity data unusable. The slope of the NRM/PTRM line is the paleofield/laboratory field ratio. The slopes have been converted into estimates of paleointensity H_a.*

Thellier, E. and Thellier, O., 1959. Sur l'intensité du champ magnétique terrestre dans le passé historique et géologique: Ann. Géophys., v. 15, p. 275-376.

West, G.F. and Dunlop, D.J., 1971. An improved ballistic magnetometer for rock magnetic experiments: J. Sci. Instrum., v. 4, p. 37-40.